

A new interface cement equilibrated mortar method with Ventcel conditions

Caroline Japhet¹, Yvon Maday², and Frédéric Nataf³

1 Introduction

For many applications in mechanics or fluid dynamics, one need to use different discretizations in different regions of the computational domain to match with the physical scales. Mortar methods [2] are domain decomposition techniques based on a weak coupling between subdomains and enable the use of nonconforming grids. On the other hand, optimized Schwarz methods [4, 11, 9, 7, 5], based on Robin or Ventcel transmission conditions and motivated by the physics of the underlying problem, greatly enhance the information exchange between subdomains and lead to robust and fast algorithms. Moreover, the Ventcel conditions reduce dramatically the convergence factor of the Schwarz algorithm compared to Robin conditions [7, 5].

In the finite element case, the NICEM method [6, 8], a new interface cement using Robin conditions and corresponding to an equilibrated mortar approach (i.e. there is no master and slave sides) has been developed for Schwarz type methods.

In this paper we extend this approach to Ventcel conditions.

We first consider the problem at the continuous level: find u such that

$$(Id - \Delta)u = f \quad \text{in } \Omega \quad (1)$$

$$u = 0 \quad \text{on } \partial\Omega, \quad (2)$$

where Ω is a $\mathcal{C}^{1,1}$ (or convex polygon in 2D or polyhedron in 3D) domain of \mathbb{R}^d , $d = 2$ or 3 , and f is given in $L^2(\Omega)$. We assume that Ω is decomposed into K non-overlapping subdomains: $\overline{\Omega} = \cup_{k=1}^K \overline{\Omega}^k$. We suppose that the subdomains Ω^k , $1 \leq k \leq K$ are either $\mathcal{C}^{1,1}$ or polygons in 2D or polyhedrons in 3D. Let \mathbf{n}_k be the outward normal from Ω^k . We also assume that this decomposition is geometrically conforming. We introduce $\Gamma^{k,\ell}$ the interface of two adjacent subdomains, $\Gamma^{k,\ell} = \partial\Omega^k \cap \partial\Omega^\ell$. An optimized Schwarz algorithm for problem (1)-(2) is

$$\begin{aligned} (Id - \Delta)u_k^{n+1} &= f && \text{in } \Omega^k \\ u_k^{n+1} &= 0 && \text{on } \partial\Omega^k \cap \partial\Omega \\ \mathcal{B}_{k,\ell}(u_k^{n+1}) &= \mathcal{B}_{k,\ell}(u_\ell^n) && \text{on } \Gamma^{k,\ell} \end{aligned}$$

¹ Université Paris 13, LAGA, UMR 7539, F-93430, Villetaneuse, France. INRIA Paris-Rocquencourt, BP 105, 78153 Le Chesnay, France, e-mail: japhet@math.univ-paris13.fr · ² UPMC Univ Paris 06, UMR 7598, Laboratoire Jacques-Louis Lions, F-75005, Paris, France. Institut Universitaire de France. Brown Univ, Division of Applied Maths, Providence, RI, USA, e-mail: maday@ann.jussieu.fr · ³ UPMC Univ Paris 06, UMR 7598, Laboratoire Jacques-Louis Lions, F-75005, Paris, France, e-mail: nataf@ann.jussieu.fr

where $(\mathcal{B}_{k,\ell})_{1 \leq k, \ell \leq K, k \neq \ell}$ is the chosen transmission operator on the interface between subdomains Ω^k and Ω^ℓ :

$$\begin{aligned} \text{Robin case: } \mathcal{B}_{k,\ell} \varphi &= \partial_{\mathbf{n}} \varphi + \alpha \varphi \\ \text{Ventcel case: } \mathcal{B}_{k,\ell} \varphi &= \partial_{\mathbf{n}} \varphi + \alpha \varphi - \beta \Delta_{\tau_{k,\ell}} \varphi, \end{aligned}$$

where $\Delta_{\tau_{k,\ell}}$ stands for the Laplace-Beltrami operator on $\Gamma^{k,\ell}$, and $\alpha, \beta > 0$ are given. In order to match Ventcel conditions in the non-conforming discrete case, we need to introduce a new independent entity representing the normal derivative of the solution on the interface as in the NICEM method [6, 8]. We thus use a Petrov Galerkin approach instead of Galerkin approximations as in standard mortar methods.

In Sect. 2 we recall the method at the continuous level. Then in Sect. 3, we present the method in the non-conforming discrete case and the discrete algorithm with Ventcel transmission conditions. We finally present in Sect. 4 simulations for two and twenty-five subdomains. The numerical analysis will be done in future paper.

2 Definition of the problem

The variational statement of the problem (1)-(2) is: Find $u \in H_0^1(\Omega)$ such that

$$\int_{\Omega} (\nabla u \nabla v + uv) dx = \int_{\Omega} f v dx, \quad \forall v \in H_0^1(\Omega). \quad (3)$$

We introduce the space $H_*^1(\Omega^k)$ defined by

$$H_*^1(\Omega^k) = \{\varphi \in H^1(\Omega^k), \varphi = 0 \text{ over } \partial\Omega \cap \partial\Omega^k\}.$$

In order to glue non-conforming grids with Ventcel transmission conditions, denoting by \underline{v} the K -tuple (v_1, \dots, v_K) , we introduce the following constrained space,

$$\begin{aligned} \mathcal{V} = \{(\underline{v}, \underline{q}) \in \left(\prod_{k=1}^K H_*^1(\Omega^k) \right) \times \left(\prod_{k=1}^K H^{-1/2}(\partial\Omega^k) \right), \\ v_k = v_\ell \text{ and } q_k = -q_\ell \text{ over } \Gamma^{k,\ell}, \forall k, \ell\}. \end{aligned} \quad (4)$$

Then, problem (3) is equivalent to the following one [8]: Find $(\underline{u}, \underline{p}) \in \mathcal{V}$ such that

$$\begin{aligned} \sum_{k=1}^K \int_{\Omega^k} (\nabla u_k \nabla v_k + u_k v_k) dx - \sum_{k=1}^K \int_{H^{-1/2}(\partial\Omega^k)} \langle p_k, v_k \rangle_{H^{1/2}(\partial\Omega^k)} \\ = \sum_{k=1}^K \int_{\Omega^k} f_k v_k dx, \quad \forall \underline{v} \in \prod_{k=1}^K H_*^1(\Omega^k). \end{aligned}$$

Being equivalent with (1)-(2), where $p_k = \partial_{\mathbf{n}_k} u$ over $\partial\Omega^k$, this problem is well posed.

Let us describe the method in the non-conforming discrete case.

3 Non-conforming discrete case with Ventcel conditions

3.1 Local problem

We introduce now the discrete spaces. Each Ω^k is provided with its own mesh \mathcal{T}_h^k , such that $\overline{\Omega}^k = \cup_{T \in \mathcal{T}_h^k} T$, $1 \leq k \leq K$. For $T \in \mathcal{T}_h^k$, let h_T be the diameter of T and h the discretization parameter: $h = \max_{1 \leq k \leq K} h_k$ with $h_k = \max_{T \in \mathcal{T}_h^k} h_T$. We suppose that \mathcal{T}_h^k is uniformly regular and that the sets belonging to the meshes are of simplicial type (triangles or tetrahedra). Let $\mathcal{P}_M(T)$ denote the space of all polynomials defined over T of total degree less than or equal to M . The finite elements are of lagrangian type, of class \mathcal{C}^0 . We define over each Ω^k two conforming spaces Y_h^k and X_h^k by: $Y_h^k = \{v_{h,k} \in \mathcal{C}^0(\overline{\Omega}^k), v_{h,k}|_T \in \mathcal{P}_M(T), \forall T \in \mathcal{T}_h^k\}$, $X_h^k = \{v_{h,k} \in Y_h^k, v_{h,k}|_{\partial\Omega^k \cap \partial\Omega} = 0\}$. The space of traces over each $\Gamma^{k,\ell}$ of elements of Y_h^k is a finite element space denoted by $\mathcal{Y}_h^{k,\ell}$. With each interface $\Gamma^{k,\ell}$, we associate a subspace $\tilde{W}_h^{k,\ell}$ of $\mathcal{Y}_h^{k,\ell}$ in the same spirit as in the mortar element method [2] in 2D or [3, 1] for a P_1 -discretization in 3D.

More precisely, let \mathcal{I} be the restriction to $\Gamma^{k,\ell}$ of the triangulation \mathcal{T}_h^k . In 2D, \mathcal{I} has two end points that we denote as $x_0^{k,\ell}$ and $x_n^{k,\ell}$ that belong to the set of vertices of the corresponding triangulation of $\Gamma^{k,\ell}$: $x_0^{k,\ell}, x_1^{k,\ell}, \dots, x_{n-1}^{k,\ell}, x_n^{k,\ell}$. The space $\tilde{W}_h^{k,\ell}$ is then the subspace of those elements of $\mathcal{Y}_h^{k,\ell}$ that are polynomials of degree $\leq M-1$ over both $[x_0^{k,\ell}, x_1^{k,\ell}]$ and $[x_{n-1}^{k,\ell}, x_n^{k,\ell}]$.

In 3D, we suppose that all the vertices of the boundary of $\Gamma^{k,\ell}$ are connected to zero, one, or two vertices in the interior of $\Gamma^{k,\ell}$. Let \mathcal{V} , \mathcal{V}_0 , $\partial\mathcal{V}$ denote respectively the set of all the vertices of \mathcal{I} , the vertices in the interior of $\Gamma^{k,\ell}$, and the vertices on the boundary of $\Gamma^{k,\ell}$. Let $S(\mathcal{I})$ be the space of piecewise linear functions with respect to \mathcal{I} which are continuous on $\Gamma^{k,\ell}$ and vanish on its boundary. We denote by Φ_a , $a \in \mathcal{V}$ the finite element basis functions. Thus, $S(\mathcal{I}) = \text{span}\{\Phi_a : a \in \mathcal{V}_0\}$. For $a \in \mathcal{V}$, let $\sigma_a := \cup\{T \in \mathcal{I} : a \in T\}$, $\mathcal{N}_a := \{b \in \mathcal{V}_0 : b \in \sigma_a\}$, and $\mathcal{N} := \cup_{a \in \partial\mathcal{V}} \mathcal{N}_a$. Let \mathcal{T}_c be the set of triangles $T \in \mathcal{I}$ which have all their vertices on the boundary of $\Gamma^{k,\ell}$. For $T \in \mathcal{T}_c$, we denote by c_T the only vertex of T that has no interior neighbor. Let \mathcal{N}_c denote the vertices a_T of \mathcal{N} which belong to a triangle adjacent to a triangle $T \in \mathcal{T}_c$. We introduce $\hat{\Phi}_a$ defined as follows:

$$\hat{\Phi}_a := \begin{cases} \Phi_a, & a \in \mathcal{V}_0 \setminus \mathcal{N} \\ \Phi_a + \sum_{b \in \partial\mathcal{V} \cap \sigma_a} A_{b,a} \Phi_b, & a \in \mathcal{N} \setminus \mathcal{N}_c \\ \Phi_{a_T} + \sum_{b \in \partial\mathcal{V} \cap \sigma_{a_T}} A_{b,a_T} \Phi_b + \Phi_{c_T}, & a = a_T \in \mathcal{N}_c \end{cases}.$$

The weights are defined such that [3]: $A_{c,a} + A_{c,b} = 1$ and $|T_{2,b}|A_{c,a} = |T_{2,a}|A_{c,b}$, for all boundary nodes $c \in \partial\mathcal{V}$ connected to two interior nodes a and b . Here $T_{2,a}$ (resp. $T_{2,b}$) denote the adjacent triangle to abc having a (resp. b) as a vertex and its

two others vertices on $\partial\mathcal{V}$. For all boundary nodes $c \in \partial\mathcal{V}$ connected to only one interior node a , the weights are $A_{c,a} = 1$.

The space $\tilde{W}_h^{k,\ell}$ is then defined by $\tilde{W}_h^{k,\ell} := \text{span} \{ \hat{\Phi}_a, a \in \mathcal{V}_0 \}$. Then \tilde{W}_h^k is the product space of the $\tilde{W}_h^{k,\ell}$ over each ℓ such that $\Gamma^{k,\ell} \neq \emptyset$.

We introduce now the discrete problem. Let $\nabla_{\tau_{k,\ell}}$ be the gradient operator on $\Gamma^{k,\ell}$. We define the discrete constrained space as follows:

$$\begin{aligned} \mathcal{V}_h = \{ (\underline{u}_h, \underline{p}_h) \in \left(\prod_{k=1}^K X_h^k \right) \times \left(\prod_{k=1}^K \tilde{W}_h^k \right), \\ \int_{\Gamma^{k,\ell}} ((p_{h,k} + \alpha u_{h,k}) - (-p_{h,\ell} + \alpha u_{h,\ell})) \psi_{h,k,\ell} + \int_{\Gamma^{k,\ell}} \beta \nabla_{\tau_{k,\ell}} (u_{h,k} - u_{h,\ell}) \nabla_{\tau_{k,\ell}} \psi_{h,k,\ell} \\ - \int_{\partial\Gamma_{k,\ell}} \beta (\nabla_{\tau_{k,\ell}} u_{h,k} - \nabla_{\tau_{k,\ell}} u_{h,\ell}) \psi_{h,k,\ell} = 0, \forall \psi_{h,k,\ell} \in \tilde{W}_h^{k,\ell} \}, \end{aligned} \quad (5)$$

and the discrete problem is the following one : Find $(\underline{u}_h, \underline{p}_h) \in \mathcal{V}_h$ such that

$$\begin{aligned} \forall \underline{v}_h = (v_{h,1}, \dots, v_{h,K}) \in \prod_{k=1}^K X_h^k, \\ \sum_{k=1}^K \int_{\Omega^k} (\nabla u_{h,k} \nabla v_{h,k} + u_{h,k} v_{h,k}) dx - \sum_{k=1}^K \int_{\partial\Omega^k} p_{h,k} v_{h,k} ds = \sum_{k=1}^K \int_{\Omega^k} f_k v_{h,k} dx. \end{aligned} \quad (6)$$

Let us describe the algorithm in the discrete case.

3.2 Iterative algorithm

We restrict ourselves to the presentation of the algorithm in 2D.

The recommended approach to find the solution of the previous discrete problem is a GMRES acceleration [12] of the iterative Schwarz algorithm. For the sake of clarity, let us present the plain Jacobi algorithm applied to the discrete Schwarz algorithm : let $(u_{h,k}^n, p_{h,k}^n) \in X_h^k \times \tilde{W}_h^k$ be a discrete approximation of (u, p) in Ω^k at step n . Then, $(u_{h,k}^{n+1}, p_{h,k}^{n+1})$ is the solution in $X_h^k \times \tilde{W}_h^k$ of

$$\begin{aligned} \int_{\Omega^k} (\nabla u_{h,k}^{n+1} \nabla v_{h,k} + u_{h,k}^{n+1} v_{h,k}) dx - \int_{\partial\Omega^k} p_{h,k}^{n+1} v_{h,k} ds = \int_{\Omega^k} f_k v_{h,k} dx, \forall v_{h,k} \in X_h^k, \quad (7) \\ \int_{\Gamma^{k,\ell}} ((p_{h,k}^{n+1} + \alpha u_{h,k}^{n+1}) \psi_{h,k,\ell} + \beta \nabla_{\tau_{k,\ell}} u_{h,k}^{n+1} \nabla_{\tau_{k,\ell}} \psi_{h,k,\ell}) - \int_{\partial\Gamma_{k,\ell}} \beta \nabla_{\tau_{k,\ell}} u_{h,k}^{n+1} \psi_{h,k,\ell} \\ = \int_{\Gamma^{k,\ell}} ((-p_{h,\ell}^n + \alpha u_{h,\ell}^n) \psi_{h,k,\ell} + \beta \nabla_{\tau_{k,\ell}} u_{h,\ell}^n \nabla_{\tau_{k,\ell}} \psi_{h,k,\ell}) \\ - \int_{\partial\Gamma_{k,\ell}} \beta \nabla_{\tau_{k,\ell}} u_{h,\ell}^n \psi_{h,k,\ell}, \quad \forall \psi_{h,k,\ell} \in \tilde{W}_h^{k,\ell}. \end{aligned} \quad (8)$$

An initial guess $(g_{k,\ell})$ is given on each interface $\Gamma_{k,\ell}$, and by convention for the first iterate, the right-hand side in (8) is given by $g_{k,\ell}$.

4 Numerical results

In this part, we consider a P_1 finite element approximation. Problem (6) is a square linear system, invertible in the various numerical tests we performed, the results presented below being some of them. We study the numerical error analysis for problem (6), as well as the convergence of the algorithm (7)-(8) with Ventcel compared to Robin (i.e. $\beta = 0$) transmissions conditions.

We consider the initial problem with exact solution $u(x,y) = x^3y^2 + \sin(xy)$. The domain is the unit square $\Omega = (0,1) \times (0,1)$.

We decompose Ω into non-overlapping subdomains with meshes generated in an independent manner. On Fig. 1, we consider the case of 2 non-conforming meshes (on the left), and the case of 25 non-conforming meshes (on the right). In the sequel, for the error curves versus h , the computed solution is the solution at convergence of the discrete algorithm (7)-(8), with a stopping criterion on the L^2 norm of the jumps of the interface conditions that must be smaller than 10^{-14} .

4.1 Choice of the Ventcel parameters α, β

In our numerical results, the Ventcel parameters are obtained by minimizing the convergence factor (depending on the mesh size in that case). In the conforming two subdomains case, with constant mesh size h and an interface of length L , the optimal theoretical values of the Ventcel parameters α, β which minimize the convergence

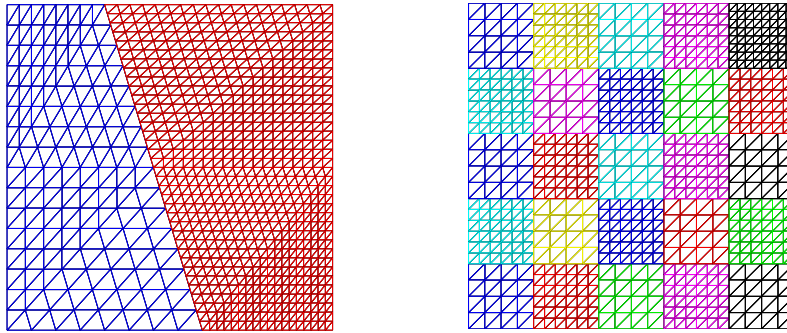


Fig. 1 Nonconforming domain decomposition in 2 domains (left), and 25 domains (right)

factor at the continuous level are [5]:

$$\alpha^* = \frac{k_{max}^2 \sqrt{k_{min}^2 + 1} - k_{min}^2 \sqrt{k_{max}^2 + 1}}{\sqrt{2(k_{max}^2 - k_{min}^2)} \left((\sqrt{k_{max}^2 + 1} - \sqrt{k_{min}^2 + 1}) \left((k_{max}^2 + 1) \sqrt{k_{min}^2 + 1} - (k_{min}^2 + 1) \sqrt{k_{max}^2 + 1} \right) \right)^{\frac{1}{4}}} \quad (9)$$

$$\beta^* = \frac{\sqrt{k_{max}^2 + 1} - \sqrt{k_{min}^2 + 1}}{\sqrt{2(k_{max}^2 - k_{min}^2)} \left((k_{max}^2 + 1) \sqrt{k_{min}^2 + 1} - (k_{min}^2 + 1) \sqrt{k_{max}^2 + 1} \right)^{\frac{3}{4}}},$$

where k_{min} and k_{max} are respectively the minimum and maximum frequencies which can be represented on a grid with mesh size h , given by $k_{min} = \frac{1}{L}$ and $k_{max} = \frac{\pi}{h}$. In the non-conforming case, the mesh size is different for each side of the interface. Thus, we consider the parameters given by (9) with $h = h_m$ denoted by (α^m, β^m) , or with $h = h_M$ denoted by (α^M, β^M) , where h_m and h_M are respectively the smallest and highest step size on the interface. We consider also the Robin case with the optimal theoretical value given by [5]: $\alpha_R^* = \left(\left(\frac{\pi}{L} \right)^2 + 1 \right) \left(\left(\frac{\pi}{h_M} \right)^2 + 1 \right)^{\frac{1}{4}}$.

4.2 Two subdomains case

In this part we consider the 2 non-conforming meshes on the left of Fig. 1. As the problem (6) depends on α, β , we consider two cases: $(\alpha, \beta) = (\alpha_m, \beta_m)$ (case (m)) and $(\alpha, \beta) = (\alpha_M, \beta_M)$ (case (M)). In order to observe the error versus h , a computed solution (solution of (6)) corresponds to the solution at convergence of (7)-(8). The solution with $(\alpha, \beta) = (\alpha_m, \beta_m)$ is different from the one with $(\alpha, \beta) = (\alpha_M, \beta_M)$. We represent on Fig. 2 (left), for both cases, the relative H^1 error (defined as in [8]), and the relative L^2 error versus the mesh size h , in logarithmic scale. We start from the 2 non-conforming meshes and then refine successively each mesh by dividing the mesh size by two. We observe similar results for both cases. The results show that the relative H^1 error tends to zero at the same rate as the mesh size h . We also observe that the relative L^2 error tends to zero at the same rate as h^2 . We represent on Fig. 2 (right) the asymptotic performance with optimized Ventcel (i.e. $\alpha = \alpha_M, \beta = \beta_M$) or Robin (i.e. $\alpha = \alpha_R^*, \beta = 0$) conditions, for the Schwarz algorithm (7)-(8) and for the GMRES algorithm. We simulate directly the error equations, $f = 0$, and use a random initial guess so that all the frequency components are present. We plot the number n_* of iterations (taken to reduce the error by a factor 10^{-6}) versus h on a log-log plot. The numerical results show the asymptotic behavior predicted by the analysis given in [5]:

- $n_* = O(h^{\frac{1}{2}})$ for Robin (i.e. $\alpha = \alpha_R^*, \beta = 0$) with Schwarz as an iterative solver,
- $n_* = O(h^{\frac{1}{4}})$ for Robin with GMRES (i.e. Schwarz used as a preconditioner),
- $n_* = O(h^{\frac{1}{4}})$ for Ventcel (i.e. $\alpha = \alpha_M, \beta = \beta_M$) with Schwarz as an iterative solver,
- $n_* = O(h^{\frac{1}{8}})$ for Ventcel with GMRES.

We also observe that using Krylov acceleration (GMRES) improves the asymptotic performance by a square root.

4.3 Twenty-five subdomains case

We now consider the 25 non-conforming meshes on the right of Fig. 1.

In order to observe the H^1 error, each computed solution corresponds to the solution at convergence of (7)-(8). We represent on Fig. 3 (left) the relative H^1 error versus the mesh size h in logarithmic scale. We start from the 25 non-conforming meshes and then refine successively each mesh by dividing the mesh size by two. The results show that the relative H^1 error tends to zero at the same rate as the mesh size h . On Fig. 3 (right), we study the performance of the algorithm (7)-(8) with Ventcel and Robin transmission conditions. We simulate directly the error equations, $f = 0$, and use a random initial guess on the interfaces. We plot the H^1 and L^∞ errors versus the number of iterations. We observe that the number of iterations

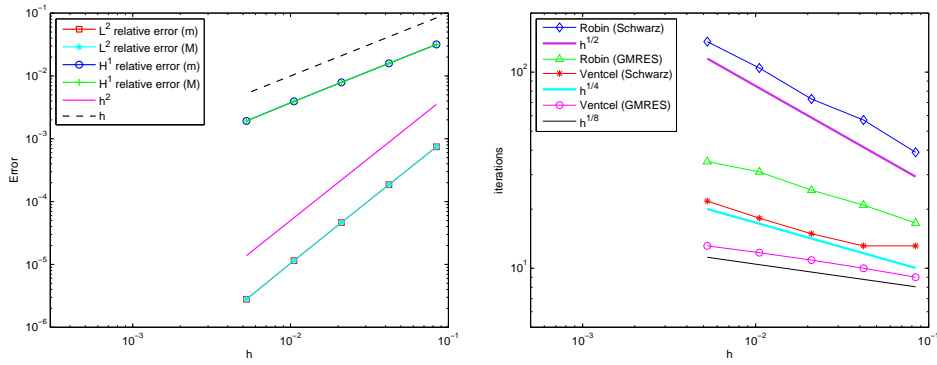


Fig. 2 Decomposition in 2 subdomains: error analysis versus h (left), and asymptotic number of iterations required by the method with optimized Robin or Ventcel conditions, when the method is used as iterative solver, or used as preconditioner for a Krylov method (GMRES)

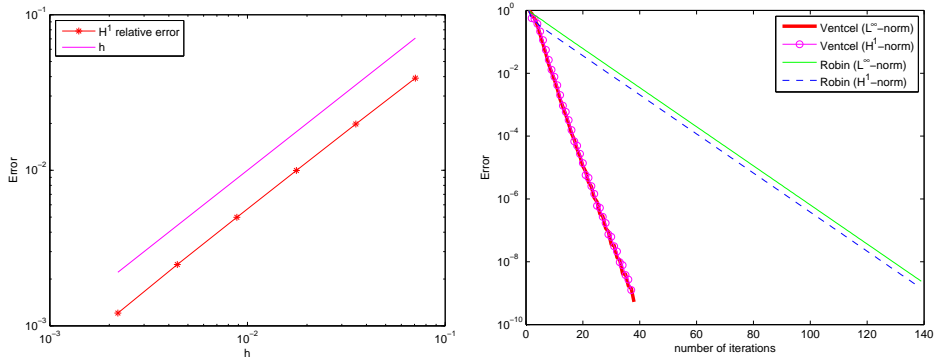


Fig. 3 Decomposition in 25 subdomains: H^1 error versus h (left), and error versus iterations (in the H^1 and L^∞ norms) with optimized Robin or Ventcel conditions

to obtain an error smaller than 10^{-6} is by a factor 4 higher with optimized Robin conditions compared to optimized Ventcel conditions. The results are similar for the H^1 and L^∞ errors.

References

1. Ben Belgacem, F., Maday, Y.: Coupling spectral and finite elements for second order elliptic three-dimensional equations. *SIAM J. Numer. Anal.* **36** (4), 1234–1263 (1999)
2. Bernardi, C., Maday, Y., Patera, A.: A new nonconforming approach to domain decomposition: the mortar element method. Brezis, H. and Lions, J.L., Pitman (1989)
3. Braess, D., Dahmen, W.: Stability estimates of the mortar finite element method for 3-dimensional problems. *East-West J. Numer. Math.* **6** (4), 249–263 (1998)
4. Desprès, B.: Domain decomposition method and the Helmholtz problem. *Mathematical and Numerical aspects of wave propagation phenomena*, SIAM, 44–52 (1991)
5. Gander, M.J.: Optimized Schwarz Methods. *SIAM J. Numer. Anal.* **44** (2), 699–731 (2006)
6. Gander, M.J., Japhet, C., Maday, Y., Nataf, F.: A New Cement to Glue Nonconforming Grids with Robin Interface Conditions : The Finite Element Case. In R. Kornhuber, R.H.W. Hoppe, J. Périaux, O. Pironneau, O.B. Widlund, J. Xu (eds) *Domain Decomposition Methods in Science and Engineering*, Lecture Notes in Computational Science and Engineering **40**, 259–266. Springer (2004)
7. Japhet, C.: Optimized Krylov-Ventcell Method. Application to Convection-Diffusion Problems. In P. Bjorstad, M. Espedal, D. Keyes (eds) *Decomposition Methods in Sciences and Engineering*, International Conference on Domain Decomposition Methods, 3-8 june 1996, Bergen (Norway), 382–389. Springer (1998)
8. Japhet, C., Maday, Y., Nataf, F.: A New Interface Cement Equilibrated Mortar (NICEM) method with Robin interface conditions: the P_1 finite element case. *M³AS* (2013)
9. Nataf, F., Rogier, F.: Factorization of the Convection-Diffusion Operator and the Schwarz Algorithm. *M³AS* **1** 67–93 (1995)
10. Nataf, F., Rogier, F., de Sturler, E.: *Domain Decomposition Methods for Fluid Dynamics. Navier-Stokes Equations and Related Nonlinear Analysis*, Sequeira, A. (eds), 367–376. Plenum Press Corporation (1995)
11. Gastaldi, F., Gastaldi, L., Quarteroni, A.: Adaptive Domain Decomposition Methods for Advection dominated Equations. *East-West J. Numer. Math.* **4**, 165–206 (1996)
12. Saad, Y.: *Iterative Methods for Sparse Linear Systems*. SIAM (2003)